HHS Public Access

Author manuscript

J Pathol. Author manuscript; available in PMC 2021 July 30.

Published in final edited form as:

J Pathol. 2021 June ; 254(2): 159–172. doi:10.1002/path.5658.

Renal deposition and clearance of recombinant poly-IgA complexes in a model of IgA nephropathy

Xinfang Xie[1,2], **Pan Liu**[1], **Li Gao**[1,3], **Xue Zhang**[4,5], **Ping Lan**[2], **Vanesa Bijol**[6], **Jicheng Lv**[4,5], **Hong Zhang**[4,5], **Jing Jin**[1,*]

[1]Feinberg Cardiovascular and Renal Research Institute, Department of Medicine – Nephrology and Hypertension, Northwestern University Feinberg School of Medicine, Chicago, IL, USA

[2]Department of Nephrology, The First Affiliated Hospital of Medical College, Xi'an Jiaotong University, Xi'an, PR China

[3]Department of Cardiology, The First Affiliated Hospital of Medical College, Xi'an Jiaotong University, Xi'an, PR China

[4]Renal Division, Department of Medicine, Peking University First Hospital, Beijing, PR China

[5]Institute of Nephrology, Peking University, Beijing, PR China

[6]Department of Pathology, Zucker School of Medicine at Hofstra/Northwell, Hempstead, NY, USA

Abstract

IgA nephropathy (IgAN) is the most common type of glomerulonephritis worldwide, which follows a chronic but nonetheless highly variable course of progression. IgA immune complexes are the primary source of renal deposits in IgAN. Apart from the presence of granular IgA1 deposits in the glomerular mesangium and mesangial hypercellularity as common features, the detailed process of IgA1 deposition and clearance in the kidney remains unclear. We sought to examine the dynamics of IgA deposition and tissue plasticity in response to deposits including their intrarenal clearance. We followed a synthetic approach to produce a recombinant fusion between IgA Fc (rIgA) and a biotin tag, which was subsequently induced with streptavidin (SA) to form an oligomeric poly-IgA mimic. Both uninduced rIgA (mono-rIgA) and polymeric SA-rIgA (poly-rIgA) were injected intravenously into Wistar rats. Plasma IgA levels and renal and liver histology were examined in a time series. In contrast to mono-rIgA, this synthetic poly-rIgA analog formed renal deposits exclusively in the glomerulus and were mostly cleared in 3 h. However, repeated daily injections for 12 days caused long-lasting and stronger glomerular IgA deposition together with IgG and complement C3, in association with mesangial cell proliferation,

*Correspondence to: J Jin, Feinberg Cardiovascular and Renal Research Institute, Department of Medicine – Nephrology and Hypertension, Northwestern University Feinberg School of Medicine, 303 E. Superior Street, Room 8-518, Chicago, IL 60611, USA. jing.jin@northwestern.edu.

Author contributions statement

XX and JJ conceived the presented idea. XX developed the study and performed the experiments. PL, LG and XZ assisted with the experiments. XX and JJ performed analyses, drafted the manuscript, and assembled the figures. VB and PL assessed the histological images and revised the draft. JL and HZ revised the manuscript. All the authors discussed the results and commented on the manuscript.

Conflict of interest statement: Northwestern University has filed a patent application on behalf of XX and JJ regarding the IgA nephropathy rat model described in this article. JJ is a cofounder of Accubit LLC, is also an advisor to QbioMed Inc. and Enlighten Biotechnology Inc, and owns shares in Mannin Research Inc. All the other authors declared no conflicts of interest.

matrix expansion, and variable degrees of albuminuria and hematuria that phenocopied IgAN. *Ex vivo*, poly-rIgA bound cultured mesangial cells and elicited cytokine production, in addition to activating plasma C3 that was consistent with the actions of IgA immune complexes in IgAN pathogenesis. Remarkably, the kidneys were able to reverse all pathologic manifestations and restore normal glomerular histology 2 weeks after injections were halted. The synthetic model showed the kinetics between the intricate balance of renal deposition and clearance, as well as glomerular plasticity towards healing. Together, the results revealed a priming effect of existing deposits in promoting stronger and longer-lasting IgA deposition to cause renal damage.

Keywords

IgA nephropathy; IgA Fc; recombinant probe; glomerular mesangial deposition; biotin-mediated oligomerization

Introduction

The most common cause of primary glomerulonephritis, IgA nephropathy (IgAN, also referred to as Berger's disease), involves complex disease processes that are not fully understood [1,2]. The major histological features are granular diffuse IgA-dominant immune deposits in intraglomerular mesangial regions, frequently associated with mesangial hypercellularity and matrix expansion [3]. The IgA deposits consist mainly of polymeric IgA1, with variable levels of complement (C3) and IgG [4]. IgA deposition tends to have diverse histological features and is associated with a spectrum of clinical severity. At the low severity end, in healthy allograft donors and non-selected autopsy series, between 3% and 24.5% of latent mesangial IgA deposition with normal histology was found [5–8]. The clinical courses range from a completely benign incidental condition to rapidly progressive kidney failure, accompanied by corresponding histological changes from nearly normal to severe proliferative glomerulonephritis with cellular crescents in IgAN. However, the process of IgA complex deposition and the underlying conditions for its diverse clinical and histologic changes remain obscure [2].

Therefore, understanding the factors contributing to the process of IgA deposition and subsequent glomerular damage will be key for developing new prognostic tools as well as disease-specific treatments, which are currently lacking. Mounting evidence suggests that IgA1 with a hypogalactosylated hinge region is prone to self-aggregation, and aberrant glycoforms may also elicit antigenicity that promotes the formation of IgA–IgG autoimmune complexes [9–13]. These poly-IgA complexes in the circulation are the main source of the kidney deposits. It should also be noted that the hinge segment of IgA1 has been found only in higher primates, which include the great apes and humans [14]. Since the critical hinge sequence that anchors the *O*-glycans is absent in experimental animals, it has been challenging to study the process of IgA deposition in animal models.

Despite the fact that mouse IgA has different molecular features from human IgA, there are spontaneous and induced models of IgA deposition in the kidney [15]. These include genetic ddY strains of mice with spontaneously developing IgA deposits and glomerular injury [16]; dietary gluten- or vomitoxin-induced high serum IgA levels with glomerular deposits [17–

19]; autoimmune models of Bcl-2, LIGHT or BAFF transgenic mice with IgA overproduction [20–22]; and transgenic expression of the human IgA receptor FcαR1/CD89 (sCD89) together with human IgA1 [23,24]. These animal models usually present high baseline IgA levels in blood and also take time to develop IgA deposits in glomeruli, making it challenging to study IgA deposition and clearance.

Here, we took a different approach and specifically constructed a recombinant IgA analog that could be artificially induced to multimerize at high efficiency. This synthetic poly-IgA, following its injection into rats, not only deposited readily in the glomerular mesangium but also induced renal and systemic responses towards its clearance. We used this model to study the dynamics of polymeric IgA deposition as well as clearance in the kidney to better understand IgAN pathogenesis and progression.

Materials and methods

Recombinant IgA construction, biotinylation, and streptavidin-induced polymerization

The DNA sequence encoding the rat IgA C_H2–C_H3 segment was fused to an N-terminus AviTag sequence (encoding the amino acids GLNDIFEAQKIEWHE). The fusion was cloned into the plasmid vector PET30a (Invitrogen, Carlsbad, CA, USA) with the addition of a 6×His purification tag. Recombinant protein production was in 200 ml culture of the BL21 (DE3) strain of *E. coli* transformed with the vector. Details for protein expression and purification are presented in supplementary material, Supplementary materials and methods.

Purified rIgA has a natural tendency to form small amounts (up to 10–20%) of oligomers following week-long storage, due to disulfide interactions. In order to reduce the interference by these oligomers, 3 h before each injection of rats, we repurified mono-rIgA using size exclusion chromatography (SEC: Superdex S-200; GE Healthcare, Piscataway, NJ, USA).

Due to its poor solubility following bacterial expression, human recombinant IgA1 (h-rIgA) was produced alternatively using a mammalian cell stable expression system. Human IgA1 C_H2–C_H3 cDNA fused to sequences encoding IL-2 signal peptide, 6×His, and AviTag in this order at the 5’-end was cloned into the plasmid vector pcDNA3 (Invitrogen, Waltham, MA, USA). h-rIgA expression in HEK293 cells and its purification are detailed in supplementary material, Supplementary materials and methods.

BirA biotin ligase was produced using the BL21 (DE3) expression system. Purified rIgA or h-rIgA protein that contained either the human or the rat IgA Fc sequence fused to an AviTag was subjected to site-directed biotinylation; then polymerization was induced by streptavidin (see supplementary material, Supplementary materials and methods) [25]. The molecular size of induced polymer rIgA was assessed using SDS-PAGE and gel filtration on a Superdex S-200 Increase 10/300 column (GE Healthcare, Milwaukee, WI, USA).

Experiments in rats

All animal studies were carried out in accordance with regulations of the National Institutes of Health for the care and use of laboratory animals and following Northwestern University IACUC protocol #: IS00009990, OLAW: A3283–01.

Mono-rIgA or streptavidin-induced poly-rIgA was injected into 10-week-old male Wistar rats (Charles River Labs, Wilmington, MA, USA) via the rat tail vein (24 Gauge stylet-guided catheter; EXELINT International, Co, Redondo Beach, CA, USA). Single bolus injections were given at 2 mg/kg. Time series blood samples were collected by tail bleeding before and after rIgA injection. To determine the kinetics of renal deposition and clearance, we performed unilateral nephrectomy to collect the right kidney at 15 min and the left kidney at 1 h after injection, or at 1 h for the first kidney and3h for the second kidney of the same rats. Long-term repeated injection doses were at 4 mg/kg, with five and four rats in groups receiving daily injections of either poly-rIgA or mono-rIgA for 12 consecutive days, respectively. Kidneys and livers were collected 24 h after the last injection. To estimate the duration required to clear the renal deposits after receiving 12 doses of poly-rIgA, we harvested the kidneys between 2 and 14 days after the last dose of poly-rIgA. Streptavidin-induced polymerized bovine serum albumin (SA-BSA) was injected into rats as a control (see supplementary material, Supplementary materials and methods).

SDS-PAGE, western blotting, and ELISA

Purified rIgA samples were either boiled in SDS-PAGE sample buffer (Bio-Rad Laboratories, Hercules, CA, USA) supplemented with or without tris(2-carboxyethyl) phosphine (TCEP) (reducing or nonreducing condition, respectively). SA-rIgA or rIgA was incubated with rat serum to test if serum IgG was co-precipitated with SA-rIgA or rIgA. Quantitative detection of rIgA in plasma and urine was performed by ELISA. Additional details are presented in supplementary material, Supplementary materials and methods.

Histopathology, creatinine, glomerular filtration rate, and urinary sediment examinations

Frozen tissues were sectioned at 4 μm for IgA, IgG, C3, BSA, and Ki67 detection; anti-collagen IV α1 and DAPI were used as counterstains. Immunofluorescence images were captured using a Nikon Ti2 Widefield microscope (Nikon Instruments Inc, Melville, NY, USA). Fixed tissues were embedded in paraffin wax and stained with periodic acid Schiff (PAS). Further details are shown in supplementary material, Supplementary materials and methods. For electron microscopy of kidney sections, the renal cortex was fixed in 2% glutaraldehyde and 4% paraformaldehyde in 0.1 M PBS buffer. Electron dense deposits and renal morphology were evaluated using transmission electron microscopy (FEI Spirit G2 TEM; FEI Company, Hillsboro, OR, USA).

Assays for serum or urinary creatinine, glomerular filtration rate (GFR) [26] (Mannheim Pharma & Diagnostics, GmbH, Mannheim, Germany), and urinary sediments are shown in supplementary material, Supplementary materials and methods.

Mesangial cell stimulation and binding of human poly-rIgA1

Primary human mesangial cells were a gift from Dr Tomoko Hayashida at Northwestern University. Details for mesangial cell stimulation and binding of human poly-rIgA1 are presented in supplementary material, Supplementary materials and methods.

In vitro complement activation assay

Either mono-rIgA or poly-rIgA was incubated with or without freshly collected rat serum prior to assessing complement activation *in vitro*. Detailed methods are presented in supplementary material, Supplementary materials and methods.

Results

Construction of recombinant IgA–biotin fusion for induction of oligomers with streptavidin

Serum IgA interacts with its cognate Fc receptor FcαR1/CD89 on mononuclear phagocytes. This process plays a key role in the clearance of IgA immune complexes, particularly by the Kupffer cells of the liver acting on circulatory complexes, and possibly also by macrophages/monocytes to clear tissue deposits [27–31]. As mice lack a homolog of the human CD89 gene (*FCAR*: Fc fragment of IgA receptor), we chose to focus on the rat, in which CD89 (*Fcar*) shares high degree of homology with the human sequence [32].

Rat IgA lacks the equivalent of the hinge region in human IgA1 heavy chain. Its Fc segment interacts with IgA receptors (Figure 1A), including CD89, to potentiate cellular and complement responses [33]. We produced Fc of rat IgA by following a recombinant fusion strategy with an N-terminus AviTag (Figure 1B). Site-directed biotinylation of the AviTag was performed using BirA ligase [25] (Figure 1B,D). Using streptavidin (SA), we artificially induced oligomerization of Fc via a stable interaction between SA and biotin (Figure 1C,D). The molecular size of the rIgA oligomer was ~300–800 kDa, as estimated by size exclusion chromatography (SEC) (Figure 1E). We considered this synthetic complex of recombinant IgA (referred to as poly-rIgA) a mimetic of naturally formed polymeric IgA that causes IgAN (supplementary material, Figure S1).

Like immunoglobulin IgA Fc, our rIgA analog adapts a duplex fold (Figure 1B). Antibody IgA that consists of two heavy chains and two light chains is conventionally referred to as monomeric IgA, whereas two IgAs further connected by a J-chain subunit are regarded as dimeric IgA [34]. To avoid any confusion in terminology, herein we refer to our rIgA duplex as mono-rIgA in reference to immunoglobulin IgA. Biotin-rIgA was induced to form a stable poly-rIgA complex with tetrameric streptavidin, consisting of ~8 rIgA subunits (Figure 1C–E). We expected this poly-rIgA analog sterically to resemble IgA complexes in its interaction with CD89 for phagocytic clearance [30,35,36]. Furthermore, via an avidity effect [37], the clustered pattern of Fc in poly-rIgA was expected to trigger immune reactivity, including activation of an alternative complement pathway, as seen by IgA immune complexes in human disease [38,39].

Kinetics of streptavidin-induced poly-rIgA following a bolus injection in rats

We sought to determine the *in vivo* response to SA-induced poly-rIgA following i.v. injection in rats (Figure 2A). To investigate the kinetics of poly-rIgA in the systemic circulation, blood samples were collected in a time series and rIgA levels were measured by ELISA. Poly-rIgA followed fast clearance from the circulation (Figure 2B). By 20 min, serum rIgA had dropped to below 5% of the levels at the beginning. After 3 h, rIgA was no longer detectable in blood.

In order to track the kinetics of poly-rIgA deposits in the kidney, two kidneys from the same rats were separately collected by performing unilateral nephrectomy at two post-injection time points, 15 min to compare with 1 h, and 1 h to compare with 3 h (Figure 2C–E). Injection of uninduced (mono-) rIgA control gave no detectable IgA signals in the kidney (supplementary material, Figure S2). In contrast, at 15 min and 1 h after poly-rIgA injection, poly-rIgA signals were detected exclusively in the glomerulus (Figure 2C–E). All glomeruli were stained, with only a slight variation in overall intensity. At higher magnification, granular deposits were seen at capillary walls and mesangial areas (Figure 2C). There was a large reduction of poly-rIgA signals after 3 h compared with 1 h (Figure 2D,E), and by 24 h, no deposits were detected in the kidney (Figure 2F). It is plausible that the majority of renal deposits formed within the first hour, and the reduction of signal intensity in the kidney by 3 h was mainly attributable to local clearance activities. Beside the noticeable reduction of staining signals, the distribution pattern of the deposits also evolved over time (Figure 2G). At 15 min, poly-rIgA formed small puncta in the glomerulus, with some appearing to be associated with capillary loops and paramesangium (Figure 2G, inset). By 1 h, the fine puncta mostly coalesced into larger aggregates, suggesting a dynamic movement of poly-rIgA deposits from the capillary wall and paramesangium to the interstitial mesangium. During this short period, PAS/hematoxylin staining of all renal sections showed no cell proliferation or other pathological changes (supplementary material, Figure S3). To further ascertain that the renal deposits were IgA-specific, we performed injection studies using biotinylated bovine serum albumin (BSA) with polymeric induction by streptavidin. Injection of this BSA polymer complex as control did not produce any kidney deposits (supplementary material, Figure S4). It should be noted that urinalysis detected little rIgA content (supplementary material, Figure S5) despite prominent glomerular deposition of streptavidin-induced rIgA. This is likely due to the large capacity of tubular reabsorption and protein catabolism.

In the liver, poly-rIgA staining first appeared in the Kupffer cells 15 min after injection along the sinusoids (Figure 2H). After an hour, prominent staining signals could be seen in hepatocytes, suggesting that Kupffer cells transported proteins to the hepatocytes across the fenestrated endothelial layer [40]. By 3 h, few/weak IgA signals were observable as poly-rIgA had been catabolized in the liver. As in the kidney, mono-rIgA had little presence in the liver (supplementary material, Figure S2D).

Renal deposition and clearance following repeated injection of poly-rIgA

Although our bolus poly-rIgA procedure has the unique advantage of examining the dynamics of clearance, the condition is different from the disease process of IgAN with a

constant presence of pathogenic poly-IgA complexes in blood (supplementary material, Figure S6). It has been theorized that IgA deposits in the glomerulus represent the equilibrium between new deposition and their clearance [41]. Having observed quick clearance of poly-rIgA in a single dose by 20 min in the circulation and mostly by 3 h in the kidney (Figure 2B,D), we next injected repeated doses every 24 h for a total of 12 days (Figure 3A). Animals were euthanized 24 h after the last injection of poly-rIgA. In stark contrast to the single dose study that showed no IgA deposits 24 h later (Figure 2F), rats that received 12 doses of SA-induced poly-rIgA had accumulated strong deposit signals in all glomeruli (Figure 3B). In addition, the repetitive injections seemed to cause fusion of deposits into larger aggregates in the mesangium, reminiscent of findings in patients with IgAN. There were also segmental granular capillary wall deposits (Figure 3B and supplementary material, Figure S7). This observation suggests a possible seeding effect of the IgA deposits that can prime the accumulation of new deposits in subsequent injection rounds. This contrasts with the liver, which had trace remaining IgA signal 24 h after the last of the 12 doses (supplementary material, Figure S8). As a negative control, daily injection of mono-rIgA for 12 days did not cause accumulation in the kidney (Figure 3D), in keeping with the understanding of IgA deposition mainly from polymerized IgA immune complexes.

Mesangial IgG co-deposition with IgA was found in all kidney tissues (Figure 3C) and complement C3 positivity was evident in two of five rats that received 12 doses of poly-rIgA (Figure 3E). In addition, we used a Ki67 antibody to detect proliferating cells. All five rats injected with poly-rIgA had Ki67-positive nuclei in their glomeruli (Figure 3F), indicating active cell proliferation. Neither non-injected controls nor mono-rIgA-injected rats showed C3 or Ki67 positivity in their glomeruli (Figure 3E,F).

Clearance of chronic poly-rIgA deposits in the kidney

Having observed the effects of repeated doses of poly-rIgA on chronic deposition, we started a new cohort of rats to study the kinetics of intrarenal clearance. As before, we began with the same 12-day injection schedule. After the last injection of poly-rIgA, we harvested individual rats either 3, 6 or 14 days afterwards, giving the animals time to recover without additional poly-rIgA loads (Figure 4A). In striking contrast to the fast clearance following single injection where by 3 h the majority of deposits had disappeared (Figure 2E), rats that had received 12 consecutive doses of poly-rIgA retained strong signals of mesangial IgA deposits for 6 days (Figure 4B,C). After the rats had recovered for 14 days without receiving new injections, low levels of IgA deposits remained detectable, albeit with greatly reduced intensity (Figure 4D). Meanwhile, glomerular IgG co-deposits also subsided (supplementary material, Figure S9).

Histopathological and urinalysis changes after repeated poly-rIgA doses

Kidney specimens were also examined following periodic acid Schiff (PAS)/hematoxylin staining (Figure 5). Compared with the mono-rIgA and the non-injected groups, rats that received 12 doses of poly-rIgA showed histological changes reminiscent of early IgAN pathology. These included overt mesangial hypercellularity and increased matrix in the glomerulus, in addition to narrowed capillary loops (Figure 5A,B, and supplementary material, Figure S10). We did not observe inflammatory cell infiltration, crescent formation,

or segmental glomerulosclerosis of the glomerulus. While two rats had protein casts and the loss of tubular brush borders, other animals did not show evidence of interstitial or tubular damage (Figure 5A and supplementary material, Figure S10).

Interestingly, PAS staining of the recovery kidney showed a normalized number of mesangial cells, reduced matrix staining signals, and normal glomerular capillary tufts (Figure 5A). These results clearly demonstrated that following the removal of chronic IgA deposits, the mesangial matrices and the capillaries were remodeled towards healing.

Transmission electron microscopy (TEM) analysis showed mesangial expansion by cells and matrices without abnormalities of podocytes or their foot processes (Figure 5C and supplementary material, Figure S11). The texture and thickness of the glomerular basement membrane (GBM) were also normal. Consistent with findings of immunofluorescence microscopy, there were large mesangial and subendothelial electron dense deposits compared with rats without any intervention (Figure 5C and supplementary material, Figure S11).

No difference of serum creatinine levels was found in rats with either poly-rIgA or mono-rIgA injection (Figure 5D), and glomerular filtration rates (GFRs) of the rats having albuminuria were in normal range as measured by transcutaneous reading of sinistrin clearance (not shown). Urine samples from two of five rats showed continuous presence of RBC, urinary casts (Figure 5E), and albuminuria calculated at ~0.5 g/l (Figure 5F).

Poly-rIgA binds and activates renal mesangial cells in culture

Poly-IgA extracted from clinical samples can stimulate cytokine production of human mesangial cells in culture [42,43]. To examine the activity of poly-rIgA to human cells, we constructed and recombinantly produced a new rIgA derived from the human IgA1 sequence with an N-terminal AviTag for biotinylation (referred to as h-rIgA1). Similar to its rat counterpart, biotinylated h-rIgA1 formed oligomers with SA (supplementary material, Figure S12A). We performed a binding assay by adding SA-induced poly-h-rIgA1 or uninduced mono-h-rIgA1 to cultured mesangial cells. The results showed that poly-h-rIgA1, but not mono-h-rIgA1, bound the cells (Figure 6A,B). Furthermore, poly-h-rIgA1 treatment of the cells stimulated IL-6 production (Figure 6C). Like rat-derived poly-rIgA, this h-rIgA1 of the human sequence was also deposited in the glomerulus and induced mesangial cell proliferation following the injections in mice (supplementary material, Figure S12B).

Poly-IgA activates complement C3

Complement C3 deposits in the glomerulus are present in the majority of IgAN patients [44], attributable to an activating surface of the IgA complexes for binding C3 convertase (C3bBb) [45]. Unlike natural poly-IgA that also contains non-IgA components such as IgG and other associated proteins, synthetically induced poly-rIgA is simpler. To elucidate the requirement of IgA's multimeric state in interactions between IgA and C3, we performed complement activation experiments by incubating either mono-rIgA or poly-rIgA with rat serum. Following Ni-NTA purification of mono-rIgA or poly-rIgA, we probed for associated C3 by western blotting. Immunoblotting showed multiple C3 fragments in association with mono-rIgA and poly-rIgA. However, the intensity of the C3cα2 band was much stronger

with poly-rIgA compared with mono-rIgA (supplementary material, Figure S13A,B), indicating that this poly-rIgA analog could directly activate C3 in serum. These results were consistent with earlier observation of C3 deposition following poly-rIgA, as opposed to mono-rIgA injections (Figure 3E).

Discussion

Although the molecular pathogenesis of IgA nephropathy remains incompletely understood, increasing evidence suggests a causal role of circulatory IgA1 immune complexes [29,46], including conditions that promote IgA complex formation [47–52]. Following a recombinant approach, we produced oligomeric rIgA that resembles native poly-IgA. This poly-rIgA analog injected into rats formed deposits in the glomerular mesangium, together with IgG and C3. We examined intrarenal clearance of poly-rIgA deposits and observed an apparent priming effect of prior deposits to facilitate the formation of new deposits that lasted 6 days. In addition to IgA deposition, mesangial proliferation and matrix expansion occurred in glomeruli. Following the clearance of poly-rIgA deposits, renal histology also improved, demonstrating glomerular plasticity and self-healing capacity.

IgA nephropathy is a chronic condition and individuals follow different clinical courses of progression. Patients with IgAN often experience disease flare-ups, as indicated by gross hematuria and proteinuria episodes during times of infection. In renal transplantation using grafts that already had latent IgA deposits [5], the deposits gradually disappear from the kidney in its non-IgAN transplant recipient [53], suggesting dynamic IgA deposition and clearance constantly occurring. As it is rare to conduct repeated biopsies for IgAN patients, the extent of balance between deposition and clearance is unclear [11,54] (see supplementary material, Figure S6A). Our model, using an inducible poly-rIgA analog, permitted us to investigate the kinetics of the balance (supplementary material, Figure S6B). Specifically, the observed priming – or seeding – effect of existing deposits in accelerating the formation of new deposits might be relevant to the basis of IgAN flare-ups, or onset IgA deposition and gross hematuria after infection in chronic IgAN patients.

Despite the distinctions between human and mouse with respect to their IgA hinge segment and CD89 gene – both are lacking in the mouse, studies using whole IgA injection in mice yielded valuable insights. Yamaji *et al* [41] injected nude mice with nephritogenic IgA extracted from ddY mice. They found deposits along the glomerular capillary starting at 1 min and gradually accumulating for the next 2 h. These deposits disappeared after 24 h. Oruc *et al* [55] found the a1KI mouse model to be prone to mesangial IgA deposition. The deposits first appeared at 2 weeks of age and intense IgA signals were detected by 3 months. However, the molecular basis for these nephritogenic IgAs is unknown. By using synthetic IgA analogs, we were able to specifically compare the potential for mono- versus poly-rIgA to form renal deposits. Our results showed that only the latter were deposited in glomeruli, likely attributable to a higher affinity of poly-rIgA to mesangial cells, in mimicking the pathogenicity of natural IgA complexes. Benefiting from a high induction efficiency in generating poly-rIgA, we achieved consistent glomerular deposition kinetics in the study.

With respect to the polymer size of rIgA needed for renal deposition, we should clarify that even our SA-induced complexes have variable numbers of rIgA subunits. Although our single-chain rIgA naturally forms a duplex – just like its natural IgA counterpart – and streptavidin binds four biotins, dimeric rIgA chains may still have their two individual biotin tags either bind the same streptavidin or separately bind two streptavidin molecules. In the latter configuration, one complex contains two streptavidins with up to $4 \times 2 - 1 = 7$ dimeric IgAs attached to them (supplementary material, Figure S14). It should also be noted that not only can natural IgA be detected in their complex forms [56,57], but our uninduced IgA analog also spontaneously aggregates into oligomers (supplementary material, Figure S15). For animal injection experiments, we had purposely repurified mono-rIgA immediately before injecting it into rats, and there was no renal deposition from mono-rIgA, in contrast to SA-induced poly-rIgA which readily formed renal deposits.

Although our experimental results showed the distinctions between mono- and poly-rIgA analogs in their affinities to the glomerular mesangium and C3, we are uncertain about the structural basis of these interactions. One possible scenario is an avidity effect of poly-IgA that collectively gathered the strength of multivalent interactions to mesangial matrices and complements [37]. Additional research is needed to further elucidate the potentially causal role of IgA complexes and pharmacological means for their disassembly as a potential treatment for IgAN.

Admittedly, our model is limited by the short duration that the synthetic analog of IgA can be administered in rats. This prevented us from examining longer-term renal response to IgA deposits. Also, the technical complexity of the daily i.v. injection schedule required for the model substantially limited our throughput. We have not been getting consistent results in producing disease phenotypes that resemble clinical IgAN, with only two out of five rats having hematuria and proteinuria. We have yet to pinpoint the cause of the variability of urinalysis results despite apparently even levels of IgA deposition across all glomeruli and across individual animals. Technical reasons cannot be ruled out. For instance, as recombinant probes were produced in *E. coli*, a trace amount of endotoxin may still be present in purified proteins, although we performed lipopolysaccharide steps to remove endotoxin. The observed variability could indicate that IgA renal deposits are generally well tolerated and only when combined with additional inflammatory triggers will they result in disease [58,59]. In addition, recombinant proteins produced in *E. coli* lack glycosylation and our construct did not include the hinge segment of IgA. Therefore, our poly-rIgA model does not resemble clinical IgAN that is associated with galactose deficiency in IgA1 (Gd-IgA1) [60]. Instead, our poly-rIgA mimetics showed that the multimeric state of rIgA alone was sufficient to cause renal deposition (Figure 2), similar to native Gd-IgA which also has a general propensity to self-aggregate [61]. To some extent, the high avidity state of the poly-rIgA complex also coalesced IgG from rat serum (supplementary material, Figure S16). The observed rIgA–IgG co-deposition in the kidney could be attributable to these interactions. By the same token, since our anti-IgA antibody cannot distinguish between exogenous rIgA and endogenous IgA in tissue staining, we could not rule out the possibility that serum IgA coalesced with rIgA deposits via avidity binding. The strength of the synthetic model is that it depicts the early events of mesangial deposition by polymeric IgA. Through timed injection of the synthetic analog, the model allowed us to delineate the intricate balance

between deposition and clearance, in which a strong priming activity of mesangial deposits in inducing new deposition, or impeding clearance, or both was observed.

Supplementary Material

Refer to Web version on PubMed Central for supplementary material.

Acknowledgements

This study was partly funded by the National Institutes of Health grant R21AI131087 to JJ, through core services and support from the Northwestern University George M. O'Brien Kidney Research Core Center (NU GoKidney), an NIH/NIDDK funded program (P30 DK114857). XX was supported by a National Natural Science Foundation of China grant (No 81800639).

References

1. Wyatt RJ, Julian BA. IgA nephropathy. N Engl J Med 2013; 368: 2402–2414. [PubMed: 23782179]
2. Lai KN, Tang SC, Schena FP, et al. IgA nephropathy. Nat Rev Dis Primers 2016; 2: 16001. [PubMed: 27189177]
3. Roberts IS. Pathology of IgA nephropathy. Nat Rev Nephrol 2014; 10: 445–454. [PubMed: 24861083]
4. Bellur SS, Troyanov S, Cook HT, et al. Immunostaining findings in IgA nephropathy: correlation with histology and clinical outcome in the Oxford classification patient cohort. Nephrol Dial Transplant 2011; 26: 2533–2536. [PubMed: 21273233]
5. Suzuki K, Honda K, Tanabe K, et al. Incidence of latent mesangial IgA deposition in renal allograft donors in Japan. Kidney Int 2003; 63: 2286–2294. [PubMed: 12753320]
6. Waldherr R, Rambausek M, Duncker WD, et al. Frequency of mesangial IgA deposits in a non-selected autopsy series. Nephrol Dial Transplant 1989; 4: 943–946. [PubMed: 2516884]
7. Nakazawa S, Imamura R, Kawamura M, et al. Difference in IgA1 O-glycosylation between IgA deposition donors and IgA nephropathy recipients. Biochem Biophys Res Commun 2019; 508: 1106–1112. [PubMed: 30553446]
8. Gaber LW, Khan FN, Graviss EA, et al. Prevalence, characteristics, and outcomes of incidental IgA glomerular deposits in donor kidneys. Kidney Int Rep 2020; 5: 1914–1924. [PubMed: 33163712]
9. Novak J, Moldoveanu Z, Renfrow MB, et al. IgA nephropathy and Henoch-Schoenlein purpura nephritis: aberrant glycosylation of IgA1, formation of IgA1-containing immune complexes, and activation of mesangial cells. Contrib Nephrol 2007; 157: 134–138. [PubMed: 17495451]
10. Suzuki H, Moldoveanu Z, Hall S, et al. IgA1-secreting cell lines from patients with IgA nephropathy produce aberrantly glycosylated IgA1. J Clin Invest 2008; 118: 629–639. [PubMed: 18172551]
11. Novak J, Julian BA, Tomana M, et al. IgA glycosylation and IgA immune complexes in the pathogenesis of IgA nephropathy. Semin Nephrol 2008; 28: 78–87. [PubMed: 18222349]
12. Barratt J, Eitner F. Glomerular disease: sugars and immune complex formation in IgA nephropathy. Nat Rev Nephrol 2009; 5: 612–614. [PubMed: 19855421]
13. Tomana M, Novak J, Julian BA, et al. Circulating immune complexes in IgA nephropathy consist of IgA1 with galactose-deficient hinge region and antiglycan antibodies. J Clin Invest 1999; 104: 73–81. [PubMed: 10393701]
14. Sumiyama K, Saitou N, Ueda S. Adaptive evolution of the IgA hinge region in primates. Mol Biol Evol 2002; 19: 1093–1099. [PubMed: 12082128]
15. Suzuki H, Suzuki Y. Murine models of human IgA nephropathy. Semin Nephrol 2018; 38: 513–520. [PubMed: 30177023]
16. Imai H, Nakamoto Y, Asakura K, et al. Spontaneous glomerular IgA deposition in ddY mice: an animal model of IgA nephritis. Kidney Int 1985; 27: 756–761. [PubMed: 4021309]

17. Coppo R, Mazzucco G, Martina G, et al. Gluten-induced experimental IgA glomerulopathy. Lab Invest 1989; 60: 499–506. [PubMed: 2709812]
18. Rostoker G, Delprato S, Petit-Phar M, et al. IgA antigliadin antibodies as a possible marker for IgA mesangial glomerulonephritis in adults with primary glomerulonephritis. N Engl J Med 1989; 320: 1283–1284. [PubMed: 2710210]
19. Pestka JJ, Moorman MA, Warner RL. Dysregulation of IgA production and IgA nephropathy induced by the trichothecene vomitoxin. Food Chem Toxicol 1989; 27: 361–368. [PubMed: 2676788]
20. Marquina R, Díez MA, López-Hoyos M, et al. Inhibition of B cell death causes the development of an IgA nephropathy in (New Zealand white × C57BL/6)F1-bcl-2 transgenic mice. J Immunol 2004; 172: 7177–7185. [PubMed: 15153542]
21. Wang J, Anders RA, Wu Q, et al. Dysregulated LIGHT expression on T cells mediates intestinal inflammation and contributes to IgA nephropathy. J Clin Invest 2004; 113: 826–835. [PubMed: 15067315]
22. McCarthy DD, Chiu S, Gao Y, et al. BAFF induces a hyper-IgA syndrome in the intestinal lamina propria concomitant with IgA deposition in the kidney independent of LIGHT. Cell Immunol 2006; 241: 85–94. [PubMed: 16987502]
23. Launay P, Grossetête B, Arcos-Fajardo M, et al. Fcα receptor (CD89) mediates the development of immunoglobulin A (IgA) nephropathy (Berger's disease). Evidence for pathogenic soluble receptor-Iga complexes in patients and CD89 transgenic mice. J Exp Med 2000; 191: 1999–2009. [PubMed: 10839814]
24. Berthelot L, Papista C, Maciel TT, et al. Transglutaminase is essential for IgA nephropathy development acting through IgA receptors. J Exp Med 2012; 209: 793–806. [PubMed: 22451718]
25. Fairhead M, Howarth M. Site-specific biotinylation of purified proteins using BirA. Methods Mol Biol 2015; 1266: 171–184. [PubMed: 25560075]
26. Schreiber A, Shulhevich Y, Geraci S, et al. Transcutaneous measurement of renal function in conscious mice. Am J Physiol Renal Physiol 2012; 303: F783–F788. [PubMed: 22696603]
27. Monteiro RC, Van De Winkel JG. IgA Fc receptors. Annu Rev Immunol 2003; 21: 177–204. [PubMed: 12524384]
28. Monteiro RC, Moura IC, Launay P, et al. Pathogenic significance of IgA receptor interactions in IgA nephropathy. Trends Mol Med 2002; 8: 464–468. [PubMed: 12383768]
29. Floege J, Moura IC, Daha MR. New insights into the pathogenesis of IgA nephropathy. Semin Immunopathol 2014; 36: 431–442. [PubMed: 24442210]
30. Ben Mkaddem S, Rossato E, Heming N, et al. Anti-inflammatory role of the IgA Fc receptor (CD89): from autoimmunity to therapeutic perspectives. Autoimmun Rev 2013; 12: 666–669. [PubMed: 23201915]
31. Boyd JK, Barratt J. Immune complex formation in IgA nephropathy: CD89 a 'saint' or a 'sinner'? Kidney Int 2010; 78: 1211–1213. [PubMed: 21116273]
32. Maruoka T, Nagata T, Kasahara M. Identification of the rat IgA Fc receptor encoded in the leukocyte receptor complex. Immunogenetics 2004; 55: 712–716. [PubMed: 14647992]
33. Mestecky J, Raska M, Julian BA, et al. IgA nephropathy: molecular mechanisms of the disease. Annu Rev Pathol 2013; 8: 217–240. [PubMed: 23092188]
34. Brandtzaeg P, Prydz H. Direct evidence for an integrated function of J chain and secretory component in epithelial transport of immunoglobulins. Nature 1984; 311: 71–73. [PubMed: 6433206]
35. van der Boog PJ, van Kooten C, de Fijter JW, et al. Role of macromolecular IgA in IgA nephropathy. Kidney Int 2005; 67: 813–821. [PubMed: 15698421]
36. Morton HC, van Egmond M, van de Winkel JG. Structure and function of human IgA Fc receptors (Fc alpha R). Crit Rev Immunol 1996; 16: 423–440. [PubMed: 8954257]
37. Kitov PI, Bundle DR. On the nature of the multivalency effect: a thermodynamic model. J Am Chem Soc 2003; 125: 16271–16284. [PubMed: 14692768]
38. Tan Y, Zhao MH. Complement in glomerular diseases. Nephrology (Carlton) 2018; 23((Suppl 4)): 11–15.

39. Thurman JM, Nester CM. All things complement. Clin J Am Soc Nephrol 2016; 11: 1856–1866. [PubMed: 27340286]
40. Sancho J, Gonzalez E, Egido J. The importance of the Fc receptors for IgA in the recognition of IgA by mouse liver cells: its comparison with carbohydrate and secretory component receptors. Immunology 1986; 57: 37–42. [PubMed: 3002970]
41. Yamaji K, Suzuki Y, Suzuki H, et al. The kinetics of glomerular deposition of nephritogenic IgA. PLoS One 2014; 9: e113005. [PubMed: 25409466]
42. Wang Y, Zhao MH, Zhang YK, et al. Binding capacity and patho-physiological effects of IgA1 from patients with IgA nephropathy on human glomerular mesangial cells. Clin Exp Immunol 2004; 136: 168–175. [PubMed: 15030528]
43. Zhu L, Zhang Q, Shi S, et al. Synergistic effect of mesangial cell-induced CXCL1 and TGF-β1 in promoting podocyte loss in IgA nephropathy. PLoS One 2013; 8: e73425. [PubMed: 24023680]
44. Tortajada A, Gutierrez E, Pickering MC, et al. The role of complement in IgA nephropathy. Mol Immunol 2019; 114: 123–132. [PubMed: 31351413]
45. Maillard N, Wyatt RJ, Julian BA, et al. Current understanding of the role of complement in IgA nephropathy. J Am Soc Nephrol 2015; 26: 1503–1512. [PubMed: 25694468]
46. Silva FG, Chander P, Pirani CL, et al. Disappearance of glomerular mesangial IgA deposits after renal allograft transplantation. Transplantation 1982; 33: 241–246. [PubMed: 7036478]
47. Suzuki H, Fan R, Zhang Z, et al. Aberrantly glycosylated IgA1 in IgA nephropathy patients is recognized by IgG antibodies with restricted heterogeneity. J Clin Invest 2009; 119: 1668–1677. [PubMed: 19478457]
48. Suzuki H, Kiryluk K, Novak J, et al. The pathophysiology of IgA nephropathy. J Am Soc Nephrol 2011; 22: 1795–1803. [PubMed: 21949093]
49. Abbad L, Monteiro RC, Berthelot L. Food antigens and transglutaminase 2 in IgA nephropathy: molecular links between gut and kidney. Mol Immunol 2020; 121: 1–6. [PubMed: 32135400]
50. Moldoveanu Z, Wyatt RJ, Lee JY, et al. Patients with IgA nephropathy have increased serum galactose-deficient IgA1 levels. Kidney Int 2007; 71: 1148–1154. [PubMed: 17342176]
51. Shimozato S, Hiki Y, Odani H, et al. Serum under-galactosylated IgA1 is increased in Japanese patients with IgA nephropathy. Nephrol Dial Transplant 2008; 23: 1931–1939. [PubMed: 18178603]
52. Zhao N, Hou P, Lv J, et al. The level of galactose-deficient IgA1 in the sera of patients with IgA nephropathy is associated with disease progression. Kidney Int 2012; 82: 790–796. [PubMed: 22673888]
53. Sofue T, Inui M, Hara T, et al. Latent IgA deposition from donor kidneys does not affect transplant prognosis, irrespective of mesangial expansion. Clin Transplant 2013; 27(Suppl 26): 14–21. [PubMed: 24299231]
54. Chen A, Yang SS, Lin TJ, et al. IgA nephropathy: clearance kinetics of IgA-containing immune complexes. Semin Immunopathol 2018; 40: 539–543. [PubMed: 30218212]
55. Oruc Z, Oblet C, Boumediene A, et al. IgA structure variations associate with immune stimulations and IgA mesangial deposition. J Am Soc Nephrol 2016; 27: 2748–2761. [PubMed: 26825533]
56. Kawata N, Kang D, Aiuchi T, et al. Proteomics of human glomerulonephritis by laser microdissection and liquid chromatography–tandem mass spectrometry. Nephrology (Carlton) 2020; 25: 351–359. [PubMed: 31707756]
57. Kojima S, Koitabashi K, Iizuka N, et al. Proteomic analysis of whole glomeruli in patients with IgA nephropathy using microsieving. Am J Nephrol 2014; 39: 36–45. [PubMed: 24434790]
58. Rops A, Jansen E, van der Schaaf A, et al. Interleukin-6 is essential for glomerular immunoglobulin A deposition and the development of renal pathology in Cd37-deficient mice. Kidney Int 2018; 93: 1356–1366. [PubMed: 29551516]
59. Makita Y, Suzuki H, Kano T, et al. TLR9 activation induces aberrant IgA glycosylation via APRIL- and IL-6-mediated pathways in IgA nephropathy. Kidney Int 2020; 97: 340–349. [PubMed: 31748116]
60. Moldoveanu Z, Suzuki H, Reily C, et al. Experimental evidence of pathogenic role of IgG autoantibodies in IgA nephropathy. J Autoimmun 2021; 118: 102593. [PubMed: 33508637]

61. Hui GK, Wright DW, Vennard OL, et al. The solution structures of native and patient monomeric human IgA1 reveal asymmetric extended structures: implications for function and IgAN disease. Biochem J 2015; 471: 167–185. [PubMed: 26268558]

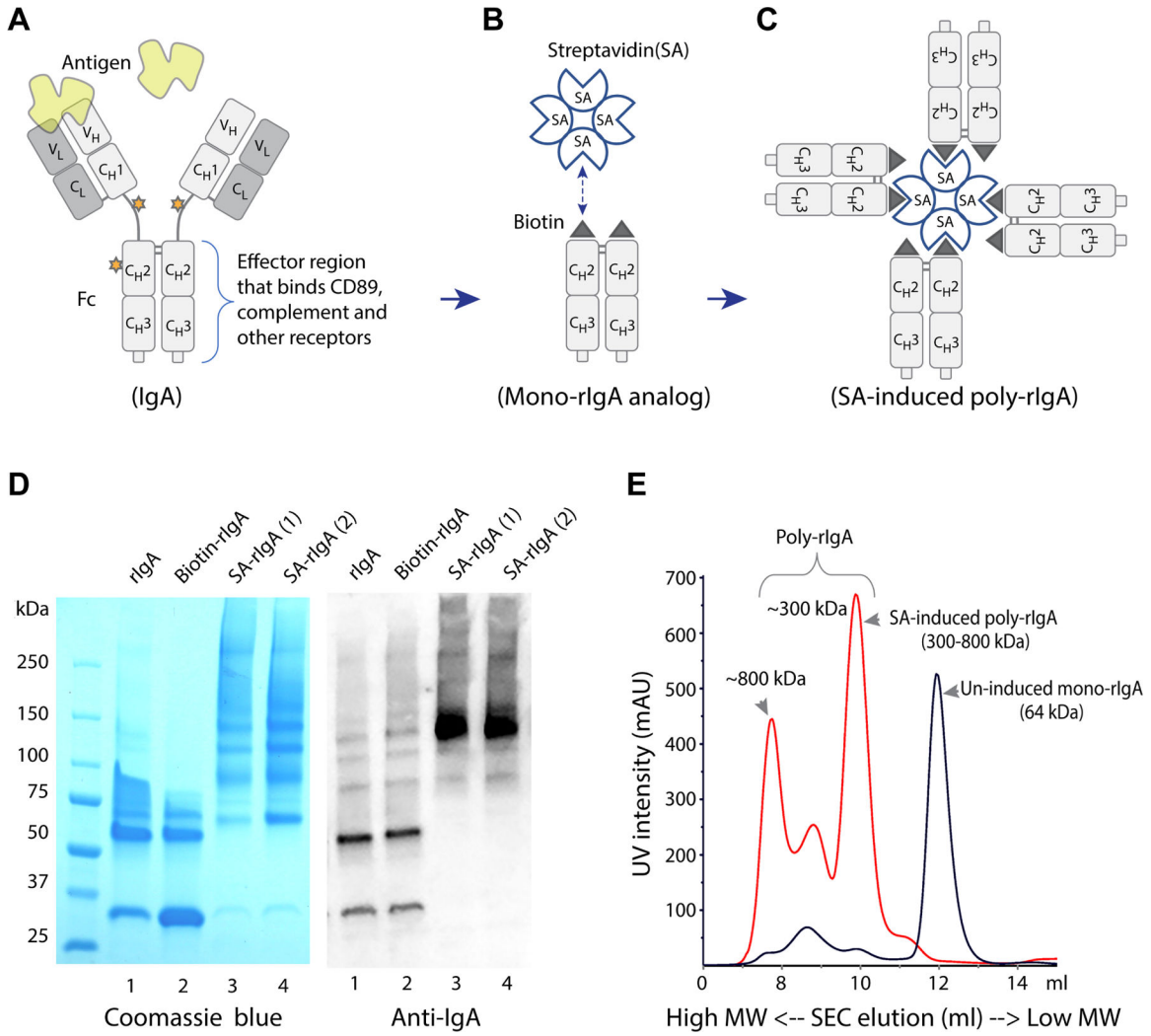

Figure 1.

Construction of the AviTag–IgA fusion protein and induction of multimerization by streptavidin. (A) The immunoglobulin IgA heavy chain is composed of variable domain VH and constant domains CH1–3 in the N- to C-terminus order. CH2 and CH3 together are referred to as the Fc segment that mediates immune reactions, including receptor binding and complement activation. The stars represent glycosylation sites. In human IgA1, the hinge region that connects CH1 and CH2 is heavily glycosylated. However, rat IgA lacks glycosylated hinge. (B) We constructed recombinant Fc of rat IgA (rIgA) with an N-terminus AviTag that was subsequently biotinylated. (C) Induction of this mono-rIgA analog with streptavidin resulted in stable poly-rIgA formation that mimics poly-IgA in IgAN. (D) Recombinant rIgA was produced in *E. coli*, and high-molecular-weight poly-rIgA formation following streptavidin (SA) induction was shown by SDS-PAGE and western blotting (left and right panels, respectively). (E) In PBS at neutral pH, the molecular sizes of mono-rIgA and streptavidin-induced poly-rIgA were compared. The size exclusion chromatography (SEC) elution sequence showed significant up (left)-shifting of poly-rIgA in molecule size from the uninduced mono-rIgA counterpart, from 64 kDa to 300–800 kDa. Several species

of poly-rIgA with distinct complex sizes existed (see comments in supplementary material, Figure S14). There were also low levels of self-aggregated rIgA of high molecular weight in uninduced rIgA (see comments in supplementary material, Figure S15).

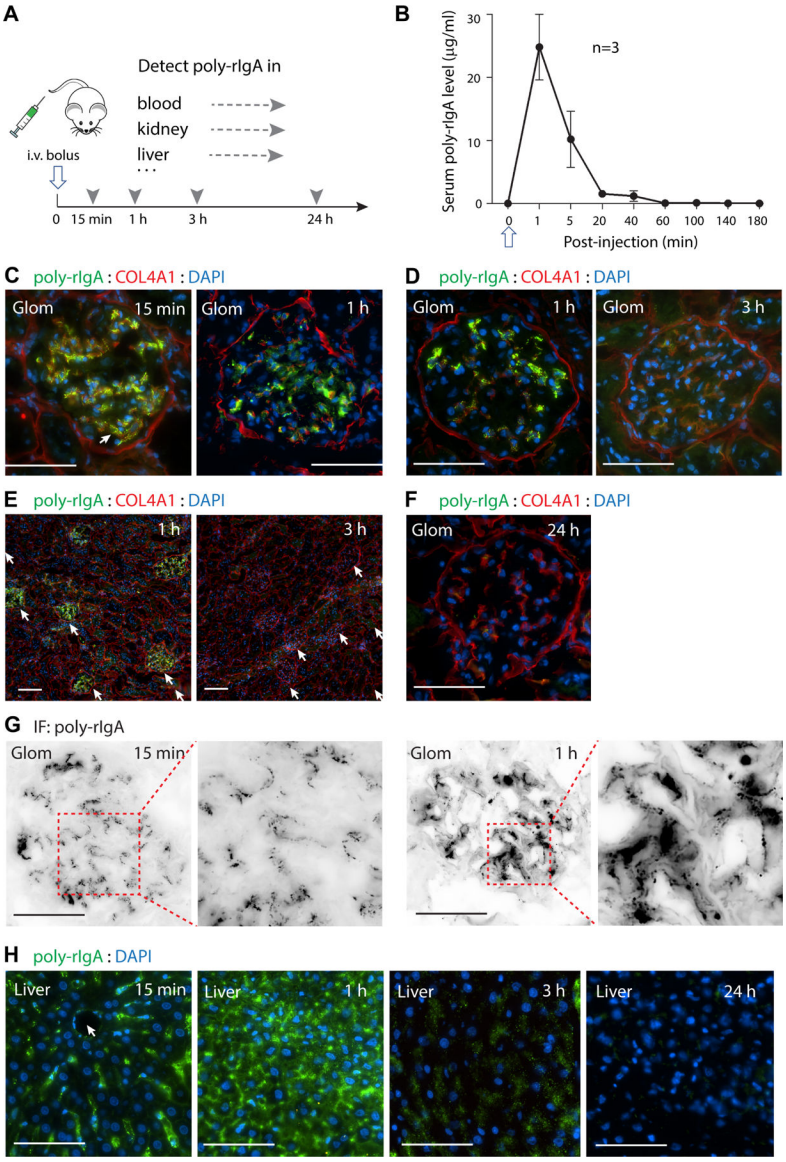

Figure 2.

Systemic and targeted deposition and clearance of poly-IgA in rats after single-dose injection. (A) A bolus i.v. injection of poly-rIgA (open arrow), or mono-rIgA control (results shown in supplementary material, Figure S2), was administered in rats. Time series samples of blood, kidney, and liver were collected at indicated times (arrowheads). Levels of rIgA in the specimens were detected using anti-IgA antibody (broken arrows). (B) Following injection, serum samples were collected by tail bleeding and the poly-rIgA contents were measured using ELISA. Following a high initial concentration, the levels dropped rapidly to below 5% after 20 min. (C, D) Comparison of poly-rIgA deposition between the two kidneys harvested at different time points from the same animal by unilateral nephrectomy. Close-up views of single glomeruli (Glom) were compared between 15 min and 1 h in C, and between 1 h and 3 h in D. Overall, there was a gradual reduction of poly-rIgA signals during this time. (E) One hour after poly-rIgA injection, signals were detected exclusively in

all glomeruli (arrows), whereas other structures such as tubules and non-glomerular blood vessels remained negative. By 3 h, the glomerular deposits were barely detectable. Scale bars: 50 μm. (F) By 24 h, poly-rIgA deposits in the glomerulus were not detectable by immunofluorescence. (G) Besides overall intensity that changed over time, there were also noticeable changes in the pattern of poly-rIgA deposits. Single channel immunofluorescence staining for poly-rIgA substantiated the differences between 15 min and 1 h. At 15 min, the deposits appeared in smaller puncta along segments of capillary walls and in paramesangial deposits. At 1 h, the deposits had coalesced into large aggregates along the mesangium (compared inset images: follow dotted boxes). (H) Poly-rIgA signals in the liver also followed time-dependent changes in terms of intensity and pattern of distribution. At 15 min, poly-rIgA staining was mostly along the direction pointing towards the central vein (arrow), consistent with the locations of the Kupffer cells along the sinusoid. By 1 and 3 h, most hepatocytes were stained positive for poly-rIgA, with a gradual decline of signal intensity over time. By 24 h, little polyrIgA was found in the liver.

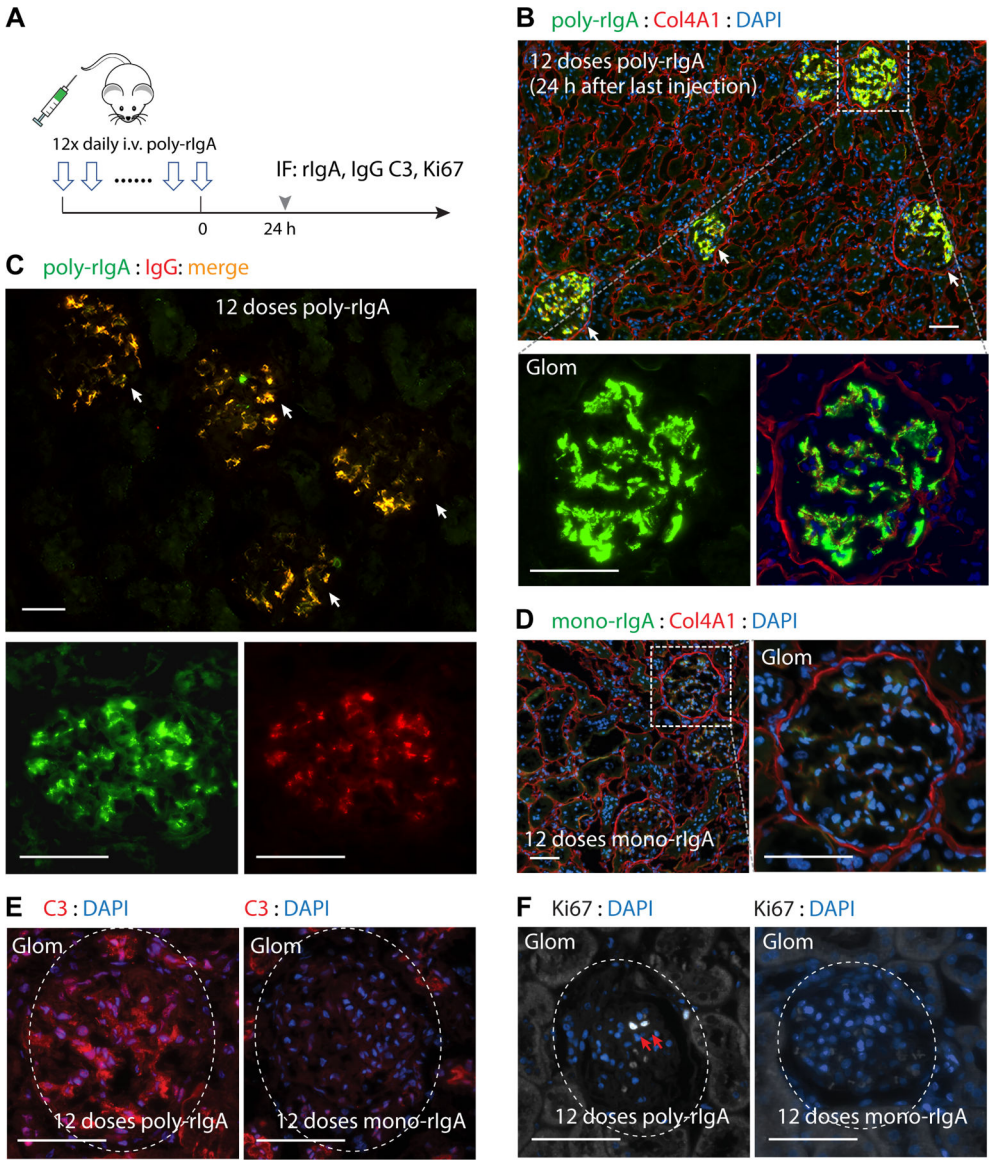

Figure 3.

Consecutive daily injections of poly-IgA induced strong and long-lasting IgA deposits in glomerular mesangium. (A) A cohort of rats was subjected to daily injection of either poly-rIgA (from SA induction) or mono-rIgA (uninduced) for 12 consecutive days. Twenty-four hours after the last injection, kidneys were collected for immunofluorescence (IF) staining to detect rIgA, IgG deposits in the kidney, complement C3, and the cell proliferation marker Ki67. (B) Rats that received poly-rIgA doses had intense staining of rIgA deposits exclusively in the glomerulus (arrows). Scale bar: 50 μm. Insets of a single glomerulus (Glom: lower panels) show that staining mainly concentrated in mesangial regions, with some on capillary walls (with Col4A1 and DAPI counterstains). (C) IgG co-deposition with IgA exclusively in the glomerular mesangium (arrows) and segmental capillary walls 24 h after 12 consecutive daily poly-rIgA injections. (D) In contrast, very weak rIgA signals along segmental capillary walls in rats that received injection of mono-rIgA (left panel:

section overview; right panel: details of a single glomerulus in the inset shown in left panel). (E) C3 deposits in the glomerulus (circled) were evident in rats injected with poly-rIgA. C3 signals were completely absent in glomeruli of mono-rIgA-injected rats (right panel), in contrast to positive signals in surrounding tubules. (F) Antibody Ki67 was used to detect nuclei of proliferating cells. Two adjacent Ki67-positive nuclei are shown (white nuclei: indicated by arrows on DAPI counterstain) in a glomerulus of poly-rIgA-injected rats. Rats that received the control injection of mono-rIgA had no Ki67-positive glomerular cells, as expected.

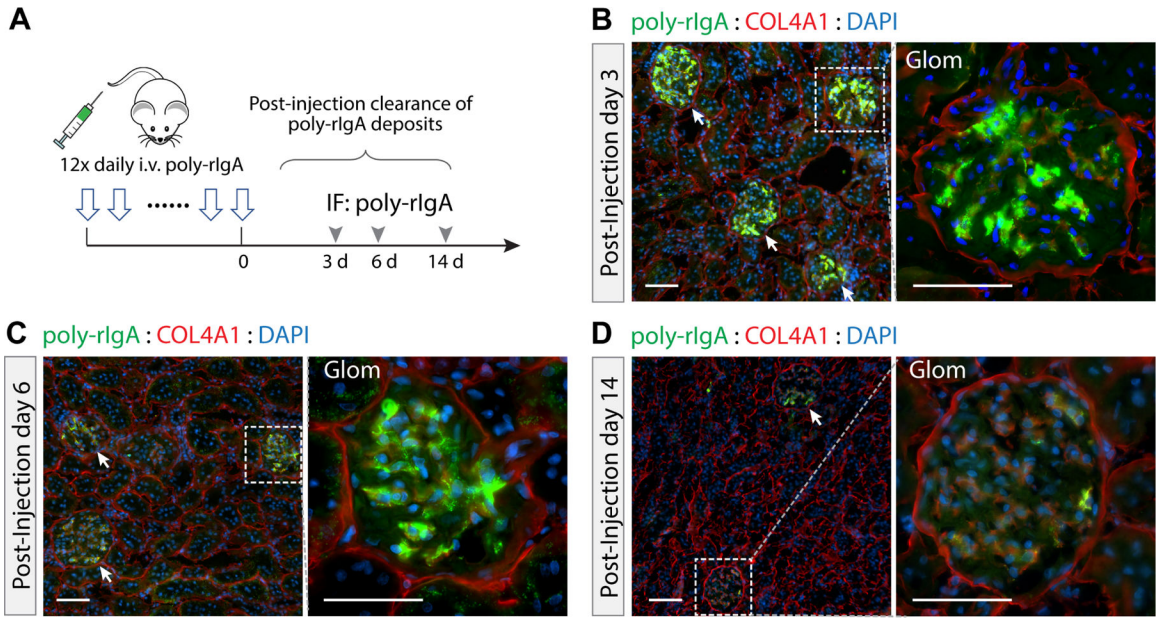

Figure 4.

Kinetics of intraglomerular clearance of poly-rIgA deposits. (A) A new cohort of rats was first treated with daily injection of poly-rIgA for 12 consecutive days. The rats were then left untreated to allow recovery during the remaining time of observation. Kidneys were collected on days 3, 6, and 14 after the last injection of poly-rIgA. (B–D) Representative examples of renal rIgA deposition are shown. Deposits stained strongly on days 3 and 6 of recovery. By day 14, only very low levels of glomerular poly-rIgA deposition were detectable.

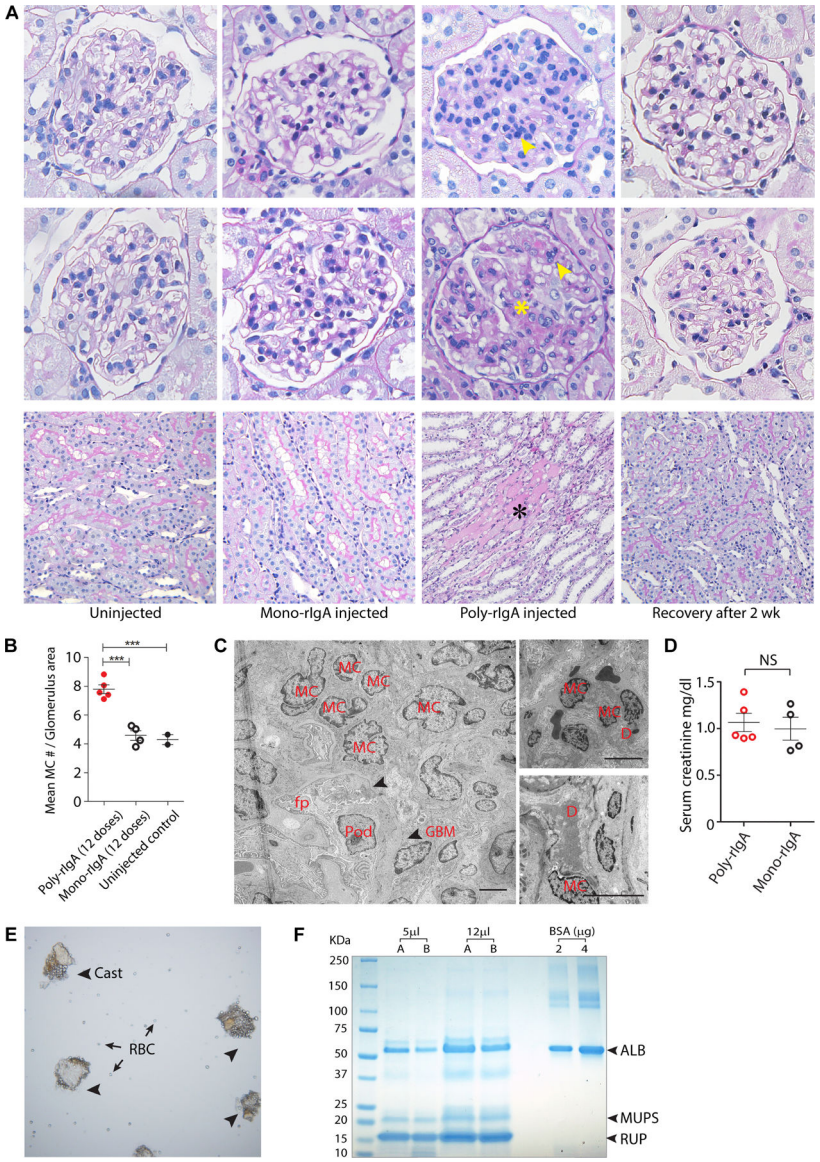

Figure 5.

Clinical and pathological features of poly-rIgA-injected rats. (A) Periodic acid Schiff (PAS)/ hematoxylin staining of rat kidney sections was performed todetect histological changes of the glomerulus following no treatment, mono-rIgA injection for 12 days, poly-rIgA injection for 12 days, or poly-rIgA injection for 12 days and recovery for an additional 14 days. For each condition, two representative examples of glomeruli are shown (top and middle). Overall, mono-rIgA-injected rats had normal-appearing glomeruli compared with untreated controls. Meanwhile, poly-rIgA injection caused histological changes of the glomerulus that resembled some of the hallmarks in IgAN, namely hypercellularity of the mesangium (yellow arrows) and matrix expansion (yellow star marking the widened purple matrices). In a particularly striking transformation, rats from poly-rIgA injection that were also allowed to recover for an additional 2 weeks showed a complete reversal of the glomerular lesions back to normal glomerulus appearance. PAS staining showed normal appearance of the tubules in

non-injected and mono-rIgA-injected rats. The brush border on the luminal side was well preserved (magenta). Two rats that received 12 doses of poly-rIgA developed tubular protein casts (black asterisk). Rats allowed to recover for 14 days showed no albuminuria (not shown) and no tubular casts (bottom). (B) Statistical analysis of hypercellularity of the mesangium among poly-rIgA-, mono-rIgA-, and non-injected groups. Mean mesangial cell number (*y*-axis) was counted with the consideration of variations of glomerulus areas in the sections. The poly-rIgA group that received 12 doses of injection had the highest numbers of glomerular mesangial cells compared with the control groups (***$p < 0.001$). (C) Transmission electron microscopy (TEM) of kidneys from rats that received 12 doses of poly-rIgA showed mesangial cell (MC) proliferation, electron-dense subendothelial deposits (upper panel, right), and mesangial deposits (lower panel, right), also visible in supplementary material, Figure S11B. GBM, glomerular basement membrane (indicated by arrowheads); D, electron dense; Pod, podocyte; fp, podocyte foot processes. Scale bar: 5 μm. (D) Serum creatinine levels were not significantly different between rats following 12 doses of poly-rIgA injection or mono-rIgA injection. NS, not significant. (E) Microscopic examination of the urinary sediments of the two albuminuric rats showed tissue clumps (arrowheads) reminiscent ofsamples from patients. In addition, red blood cells (RBC) were visible (arrows), either in isolation or inassociation with the cast structures. (F) Urinalysis by SDS-PAGE and Coomassie blue staining showed proteins in urine, including albumin (ALB), and normal low-molecular-weight urinary proteins such as MUPS and RUP. Urinary samples A and B were collected on different days from rats that received 12 doses of poly-rIgA. The quantity of urinary albumin was calculated based on bovine serum albumin (BSA) standards.

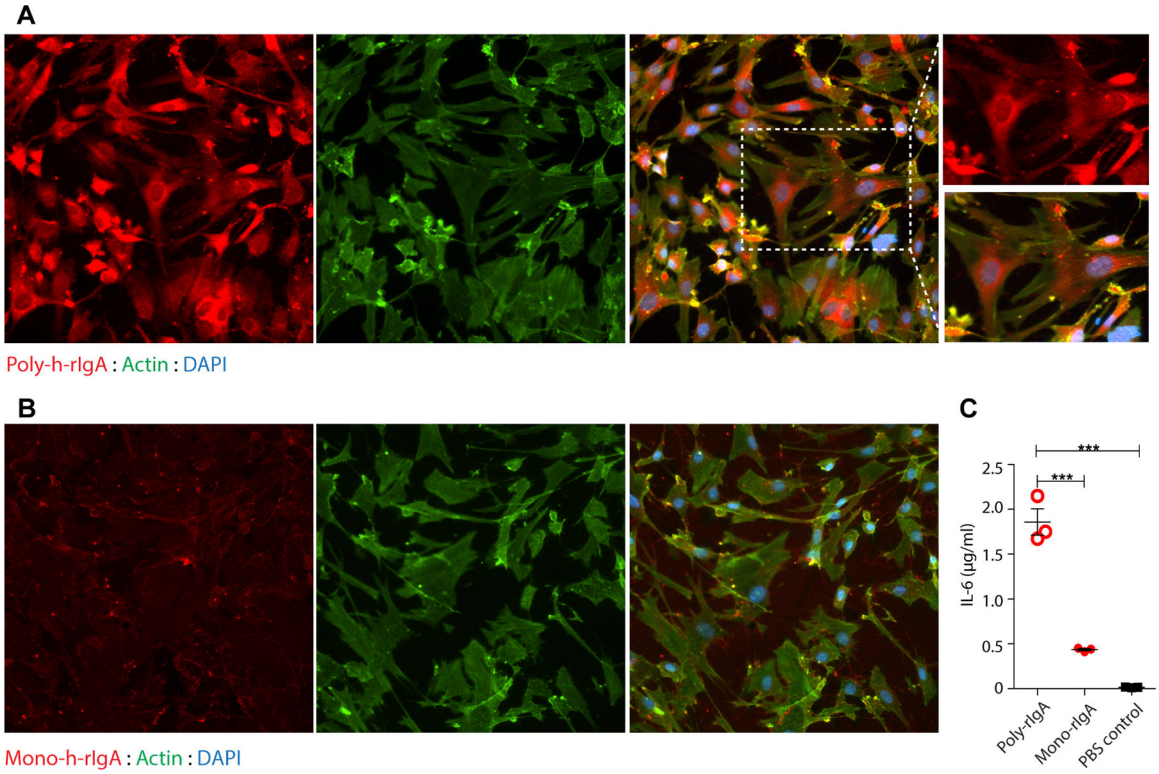

Figure 6.

Poly-IgA binds renal mesangial cells in culture. (A, B) Human glomerular mesangial cells were cultured in dishes. Human biotin-h-rIgA either in the SA-induced polymeric state (A) or in the uninduced monomeric state (B) was added to the culture medium. Following washing to remove unbound h-rIgA, the cells were fixed and then probed for IgA contents. Phalloidin staining for actin and DAPI for DNA were used as counterstains. While strong poly-h-rIgA signals were associated with the cells (in A), there was no specific binding of mono-h-rIgA detected (in B). (C) Following co-cultureofthecells with either poly- or mono-h-rIgAovernight, theculture mediumwasharvestedfor detectionof IL-6 by ELISA (*y*-axis). The inflammatory response of the cells (IL-6 production) to human poly-hrIgA was significantly greater than that to mono-h-rIgA.